Possibility of Searching for Accreting White Dwarfs with the Chinese Space Station Telescope

Wei Xie[1,2] and Hai-Liang Chen[1]

[1] Yunnan Observatories, Chinese Academy of Sciences, Kunming 650216, China; xiewei@ynao.ac.cn

[2] University of the Chinese Academy of Sciences, Beijing 100049, China

Abstract

Accreting WDs are very important for the studies of binary evolution, binary population synthesis and accretion physics. So far, there are a lot of accreting WD binaries with low accretion rates, such as cataclysmic variables, detected by different surveys. However, few accreting WD binaries with high accretion rates have been detected. In this paper, we studied the spectrum properties of accreting WD binaries and investigated whether accreting WD binaries with high accretion rates can be detected by the Chinese Space Station Telescope (CSST). We found that some accreting WD binaries with high accretion rates can be distinguishable from other types of stars with $(\mathrm{NUV} - y, \ u - y)$, $(\mathrm{NUV} - r, \ u - g)$, $(\mathrm{NUV} - i, \ u - g)$, $(\mathrm{NUV} - z, \ u - g)$ and $(\mathrm{NUV} - y, \ u - g)$ color–color diagrams. Therefore, some accreting WD binaries with high accretion rates can be detected by the CSST.

Key words: white dwarf stars: white dwarfs – binary stars: close binary stars – low mass stars: low-mass star

1. Introduction

Accreting white dwarfs (WDs) are a kind of binary systems consisting of WDs and typically main sequence (MS), Hertzsprung gap (HG) or red giant (RG) stars. They can evolve into many important objects, such as cataclysmic variables (e.g., Warner 2003), supersoft X-ray sources (e.g., van den Heuvel et al. 1992), double WDs (e.g., Iben & Tutukov 1986; Lipunov & Postnov 1988; Tutukov & Yungelson 1994; Han et al. 1995; Li et al. 2019), type Ia supernovae (Iben & Tutukov 1984; Wang & Han 2012) and binary millisecond pulsars (Taam & van den Heuvel 1986; Tauris et al. 2013). They can also evolve into AM Canum Venaticorum stars which can be detected by space borne gravitational wave detectors, such as LISA (Podsiadlowski et al. 2003; Nelemans et al. 2004; Amaro-Seoane et al. 2017; Liu et al. 2021). They are important for the studies of binary evolution, binary population synthesis, accretion physics (see Postnov & Yungelson 2014; Han et al. 2020, for a review).

The evolution of accreting WDs strongly depends on the accretion rate and WD mass (e.g., Paczynski & Zytkow 1978; Sion et al. 1979; Wolf et al. 2013; Chen et al. 2019a). It is known that there is a stable burning regime in which the accreted H-rich material will burn stably on the surface of the WDs (henceforth, stable nuclear burning white dwarfs (SNBWDs)). In this regime, the effective temperatures of the accreting WDs are about 10^5–10^6 K. They have strong emission in soft X-ray and extreme ultraviolet (EUV). If the accretion rate is smaller than the minimum rate of stable-nuclear burning, the accreted material burns unstably on the surface of WD, observable as classical novae or recurrent novae. If the accretion rate is larger than the maximum rate of stable-nuclear burning, the evolution of accreting WDs is still under debate. Cassisi et al. (1998) found that the WD will evolve into an RG star after accreting a small amount of material. However, Hachisu et al. (1996) found that optically thick wind will occur and the photospheric radius of accreting WDs will significantly expand, lowering the effective temperatures. We refer to this kind of accreting WDs as rapidly accreting WDs (RAWDs) following Lepo & van Kerkwijk (2013). The RAWDs have effective temperatures of about 10^4–10^5 K, radiating predominantly in the EUV.

From the observational side, only a very small fraction of SNBWDs can be observed as supersoft X-ray sources. So far, only tens of supersoft X-ray sources have been found in our galaxy (Kahabka & van den Heuvel 2006). However, thousands of SNBWDs are expected from theoretical studies (Chen et al. 2014). The difference of the number of SNBWDs can be partially explained as follows. The emission of SNBWDs is predominantly in soft X-ray and EUV and can be easily absorbed by the interstellar medium (Chen et al. 2014, 2015). Therefore, only a small fraction of SNBWDs can be detected. On the other hand, no RAWDs have been found so far. Only several possible RAWD candidates have been suggested, such as V Sge, Qu Carinae, WX Cen, B617Sgr, RX J0513.9-6951 and LMC N66 (Steiner & Diaz 1998; Hachisu & Kato 2003). Lepo & van Kerkwijk (2013) has attempted to search RAWDs in the central core of the Small Magnellanic Cloud from these far-UV bright sources and no RAWD candidates have been found in their search. Moreover, binary population synthesis studies (e.g., Chen et al. 2014)

suggest that there should be about 2000 RAWDs in a spiral-like galaxy with a mass of $10^{11} M_\odot$. Therefore, there is a big difference of the number of accreting WDs between the observational and theoretical studies. With this discrepancy in mind, it would be necessary to search more accreting WDs from the observational side.

The Chinese Space Station Telescope (CSST) is a 2 m space telescope and have the same orbit as the China Manned Space Station (Zhan 2011; Cao et al. 2018; Gong et al. 2019). It is scheduled to be launched at the end of 2024. This telescope has seven photometric imaging bands and three spectroscopic bands ranging from 255 to 1100 nm. It can perform photometric imaging and slit-free grating spectroscopy at the same time with a spatial resolution around 0.15″. One filter of the CSST photometric imaging survey is NUV (i.e., 255–322 nm). With this filter, there is a possibility to find bright UV sources in our galaxy or nearby galaxies, such as Large/Small Magnellanic Cloud. Given the high temperatures and luminosity of accreting WDs, in particular, SNBWDs and RAWDs, it would be interesting to know if we can find any accreting WDs with the CSST in our galaxy or nearby galaxies.

The aim of this paper is to investigate the possibility of searching accreting WD binaries (i.e., SNBWDs and RAWDs) with the CSST and provide a possible criterion to distinguish accreting WD binaries from other types of stars. The paper is organized as follows. In Section 2, we introduce the emission spectra and properties of different types of accreting WD binaries. In Section 3, we compute the colors of accreting WD binaries for the CSST and compare them with other stars with different types. We have a brief discussion and draw conclusions in Section 4 and Section 5, respectively.

2. The Properties of Accreting white Dwarf Binaries

2.1. Spectra of Accreting WDs

With the assumption of optically thick wind, Hachisu et al. (1999) studied the evolution of accreting WDs with different WD masses and accretion rates. They presented the dependence of radius and effective temperature on the accretion rate for different WD masses (see their Figures 3 and 4). For any given WD mass and accretion rate, we can get the radius and effective temperature by interpolation with these data. Then we can get the surface gravity of an accreting WD with a given WD mass and radius. In Figure 1, we show the surface gravities and effective temperatures of accreting WDs with different WD masses. From this plot, we can find that there is a rough linear relation between the logarithm of effective temperature and logarithm of surface gravity. This rough linear relation can be understood as follows. From previous studies (e.g., Chen et al. 2019a), we know that the evolution of accreting WDs mainly depends on their accretion rates. From Hachisu et al. (1999), we can find that there is a rough linear relation between the logarithm of accretion rate and the logarithm of effective

temperature or photospheric radius (see their Figures 3 and 4). Then we can fit these data with Equation (1). The coefficients for different WD masses are given in Table 1.

$$\log g = k_i \log T_{\mathrm{eff}} + c_i \qquad (1)$$

Regarding the spectra of accreting WDs, we adopt the spectra computed by Rauch et al. (2018).[3] They have adopted the non-local thermodynamic equilibrium stellar atmosphere model to compute grids of spectra for WD models with metallicity $Z = 0.02$, 0.001 and pure H. These spectra have been successfully applied to explain the spectra of novae and supersoft X-ray sources (Rauch et al. 2010; Rauch 2011). In Figure 2, we present an example of the spectrum for an accreting WD with $\log(g\ \mathrm{cm}^{-1}\ \mathrm{s}^2) = 4.0$, $T_{\mathrm{eff}} = 58{,}000$ K and pure H. Because the grid of spectra for WD models with pure H is much denser than models with solar metallicity, we adopt the grid of spectra for WD models with pure H in our calculation. Moreover, we have tested other choices of spectra grid and find that it does not significantly influence our results. There are some parameters of accreting WDs, which are not covered by this grid. We use the blackbody spectra for these accreting WDs.

2.2. Companions of Accreting WDs

In order to get the magnitudes of accreting WD binaries, we also need consider the emission from the companion stars of the accreting WDs. The typical companions of accreting WDs are MS, HG and RG stars.[4] For a given WD mass, we constrain its companion mass as follows. The upper limit of the companion star's mass will be the critical mass at which the binary system still undergoes stable mass transfer. Following Hurley et al. (2002) and Han et al. (2002), we adopt the critical mass ratio, 4.0, 5.0 and 1.5 for binaries with MS, HG, RG companions, respectively. On the other hand, if the donor mass is too small, the mass transfer rate will be smaller than the lower limit of stable burning rate. Then the system will not evolve into an SNBWD or RAWD. Therefore, we chose these systems with thermal timescale mass transfer rates larger than the minimum stable burning rate. The thermal timescale mass transfer rate ($\dot{M}_{\mathrm{th}}$) can be estimated with the following equation.

$$\dot{M}_{\mathrm{th}} = \frac{M}{\tau_{\mathrm{th}}} = \frac{2RL}{GM}, \qquad (2)$$

where M, R, L are the mass, radius and luminosity of the donor star, respectively. G is the gravitational constant. τ_{th} is the thermal timescale of the donor star (Kippenhahn et al. 2012). The minimum stable burning rate for a given WD mass can be

---

[3] http://dc.zah.uni-heidelberg.de/theossa/q/web/form
[4] In some cases, the companion stars can be He stars. In this paper, we only consider these WD binaries with H-rich companions.
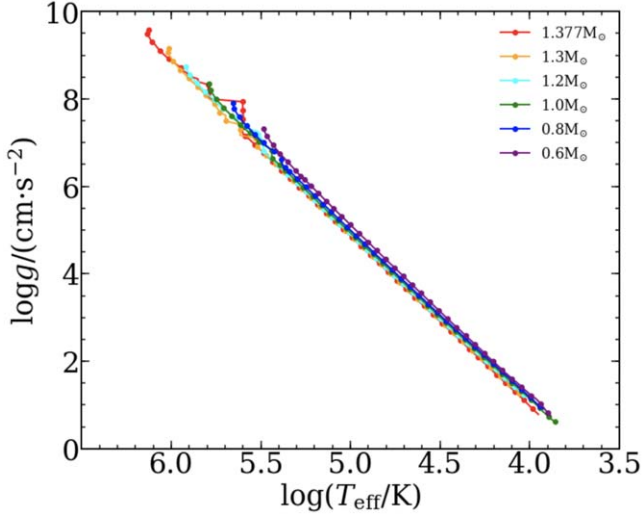
Figure 1. The surface gravities and effective temperatures of accreting WDs with different WD masses. In the plot, different colors are for different WD masses. From the upper left corner to the lower right corner, the accretion rates of accreting WDs with the same WD masses increase.

Figure 2. An example of the spectrum of an accreting WD with $\log(g\ \mathrm{cm}^{-1}\,\mathrm{s}^2) = 4.0$, $T_{\mathrm{eff}} = 58{,}000$ K and pure H (see the black line). In the plot, other lines show the intrinsic transmissions of the CSST filters. The seven bands from left to right are NUV, u, g, r, i, z, y, respectively.

Table 1
Coefficients in Equation (1) for Different WD Masses

$M_{\mathrm{WD}}/M_\odot$	1.377	1.3	1.2	1.0	0.8	0.6
k_i	3.94	3.94	3.95	3.92	3.95	3.97
c_i	14.81	14.56	14.79	14.59	14.68	14.72

given with the following equation (Chen et al. 2019a).

$$\log \dot{M}_{\mathrm{low}} = -10.35 + 8.37 \cdot M_{\mathrm{WD}} - 6.84 \cdot M_{\mathrm{WD}}^2 + 2.07 \cdot M_{\mathrm{WD}}^3, \qquad (3)$$

where M_{WD} is the WD mass in units of solar mass and $\dot{M}_{\mathrm{low}}$ is in units of $M_\odot\,\mathrm{yr}^{-1}$.

For a donor star with a given mass, we can get its effective temperature and surface gravity from the Modules for Experiments in Stellar Astrophysics isochrones and evolutionary tracks (MIST; Choi et al. 2016; Dotter 2016). In MIST, different evolutionary phases are separated. But HG and RG phases are not separated. Following Hurley et al. (2000), we separated HG and RG phases according to the stellar radius. If the radius is larger than the radius at the end of HG phase, then the star is on RG phase, otherwise on HG phase. The radius at the end of HG phase for a given mass can be calculated with the formulas in Hurley et al. (2000).

Regarding the spectra of the companions, we make use of the database YBC,[5] which provides different types of stellar libraries for stars with different types (Chen et al. 2019b). For
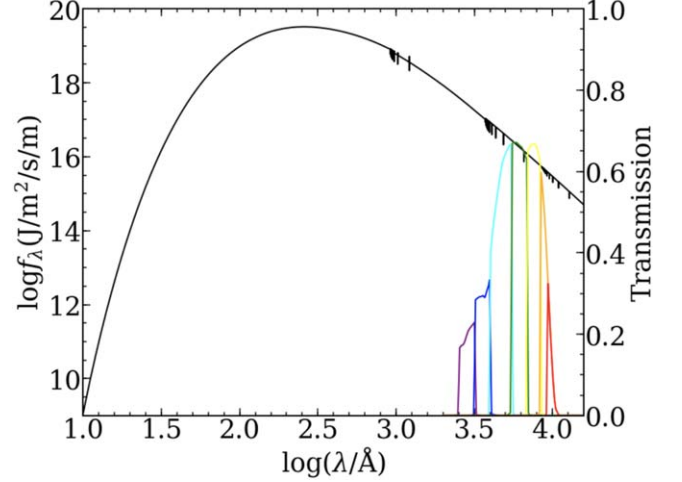
any companion star, we can select its spectra from this database according to its effective temperature and surface chemical abundances following the selection scheme in their Section 3.10.

2.3. Magnitude

For a source with observed flux f_λ, its magnitude on any i band with transmission $S_{\lambda,i}$ is given by

$$m_i = -2.5 \log \left[\frac{\int_{\lambda_1}^{\lambda_2} \lambda f_\lambda S_{\lambda,i}\,d\lambda}{\int_{\lambda_1}^{\lambda_2} \lambda f_\lambda^0 S_{\lambda,i}\,d\lambda} \right], \qquad (4)$$

where f_λ^0 is the flux of the reference object. λ_1 and λ_2 are the filter's maximum and minimum wavelength. For the CSST, AB magnitude is adopted as the reference system. The flux of reference is $f_\nu^0 = 10^{\frac{48.60}{-2.5}}\,\mathrm{erg\ s^{-1}\ cm^{-2}\ Hz^{-1}}$ (Chen et al. 2019b) and $f_\lambda^0 = \frac{c}{\lambda^2} f_\nu^0$ (c is the speed of light in a vacuum).

The absolute magnitude of the source on i band is

$$M_i = -2.5 \log \left[\left(\frac{R}{10\mathrm{pc}} \right)^2 \frac{\int_{\lambda_1}^{\lambda_2} \lambda F_\lambda 10^{-0.4A_\lambda} S_{\lambda,i}\,d\lambda}{\int_{\lambda_1}^{\lambda_2} \lambda f_\lambda^0 S_{\lambda,i}\,d\lambda} \right], \qquad (5)$$

where R is the radius of the source, A_λ is the extinction and F_λ is the intrinsic flux (Chen et al. 2019b). In this paper, we assume that the extinction is zero.

Given that the spatial resolution of the CSST is 0.15″, we can resolve a binary at 1 kpc if the binary separation is larger than 150 au, i.e., $3.2 \times 10^4\,R_\odot$. Therefore, we would expect that most binaries are unresolvable in the survey of the CSST. For
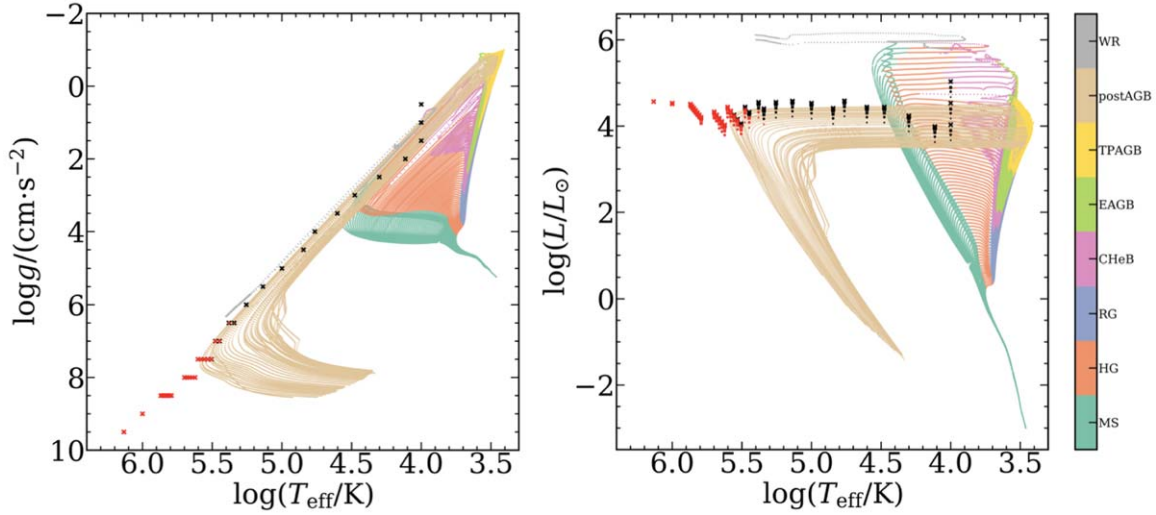
_____
[5] http://stev.oapd.inaf.it/YBC/

Figure 3. Kiel (left) and HR diagrams (right) for accreting WDs. The black and red crosses represent RAWDs and SNBWDs, respectively. Other dots in the plot shows a grid of isochrones with ages from $\log_{10}(t/\text{yr}) = 6.6$–10.1 in steps of 0.05 at solar metallicity. These isochrones are from the MIST database. Different colors in the plots indicate different types of stars (see the color bar). The explanation of these abbreviation of these stellar types are as follows. MS: main sequence, HG: Hertzsprung gap, RG: red giant, CHeB: core He burning, EAGB: early asymptotic giant branch, TPAGB: thermally pulsating AGB, WR: Wolf-Rayet.

an unresolved accreting WD binary with two components, the magnitude of the binary system can be given by the following equation.

$$m = -2.5 \log \left[\frac{\int_{\lambda_1}^{\lambda_2} \lambda f_{\lambda 1} S_{\lambda,i} d\lambda + \int_{\lambda_1}^{\lambda_2} \lambda f_{\lambda 2} S_{\lambda,i} d\lambda}{\int_{\lambda_1}^{\lambda_2} \lambda f_{\lambda}^0 S_{\lambda,i} d\lambda} \right]$$
$$= m_{1,i} - 2.5 \times \log(1 + 10^{\frac{m_{1,i}-m_{2,i}}{2.5}}), \tag{6}$$

where $f_{\lambda 1}, f_{\lambda 2}$ are the observed fluxes of the two components of the binary system, respectively. $m_{1,i}$ and $m_{2,i}$ are the magnitudes of the two components on the i band, respectively. In a similar way, we can get the absolute magnitude of the unresolved binary with the absolute magnitudes of two components.

3. Results

3.1. HR and Kiel Diagrams

In Figure 3, we show the location of accreting WDs in the Kiel and HR diagrams. From this plot, we can find that SNBWDs have higher effective temperatures and larger surface gravities compared with RAWDs. This can be understood as follows. Because SNBWDs and RAWDs have comparable H burning rates, they have comparable luminosities. For RAWDs, optically thick wind occurs (Kato & Hachisu 1994). This leads to the modest expansion of the accreting WD's photospheric radius, lowering their effective temperatures.

In order to compare these accreting WDs with other types of stars, we also plot a grid of isochrones with ages from

$\log(t/\text{yr}) = 6.6$–10.1 in 0.05 dex steps from the MIST (version 1.2) database (Choi et al. 2016; Dotter 2016). The initial stellar masses in these isochrones range from $0.1\,M_\odot$ to $73\,M_\odot$. Although the initial stellar mass can be larger than $73\,M_\odot$, we have checked that the upper limit of the mass range has little influence of our conclusions. The initial metallicity is assumed to be solar metallicity and the initial rotation velocity is $v/v_{\text{crit}} = 0.40$ (v_{crit} is the critical surface velocity). From these two plots, we can find that these accreting WDs are much brighter than these isolated WDs which have $\log(L/L_\odot) \sim (-4)$–4 and $\log(T_{\text{eff}}/\text{K}) \sim 3.5$–5.5 and are located on the cooling sequence. Their parameters are close to some post AGB stars and the central stars of planetary nebulae. These SNBWDs have relatively larger effective temperatures and surface gravities in contrast with RAWDs. In Figure 4, we also show the location of the companions of accreting WDs in the Kiel and HR diagrams. From this plot, we can find that the accreting WDs are much brighter and have higher effective temperatures compared with their companions. From Equation (6), we can find that the magnitudes of the unresolved accreting WD binary systems will be very close to the magnitudes of the accreting WDs.

3.2. Color–Color Diagrams

In order to know if we can search for accreting WDs with the CSST, we try to use different combinations of colors of the CSST and find the possible color–color diagrams to distinguish accreting WD binaries from other stars with different types. In Figure 5, we show the (NUV $- y$, $u - y$) color–color diagram for accreting WD binaries. In addition, we also show other types of stars in the same plot. Given that the possible observable
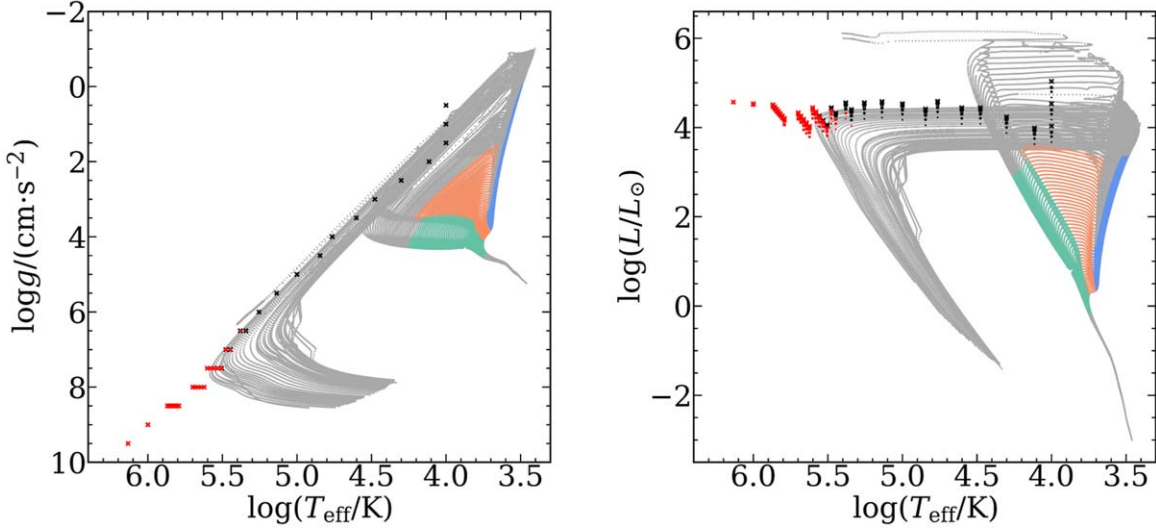
Figure 4. Kiel (left) and HR diagrams (right) for accreting WDs and their companions. The red and black crosses are for SNBWDs and RAWDs, respectively. The green, orange, blue dots are for MS, HG, RG companions of accreting WDs. The gray dots indicates the same isochrone grid as Figure 3. In order to show clearly the location of the companions of accreting WDs, we do not distinguish the stellar types in the isochrone grid.
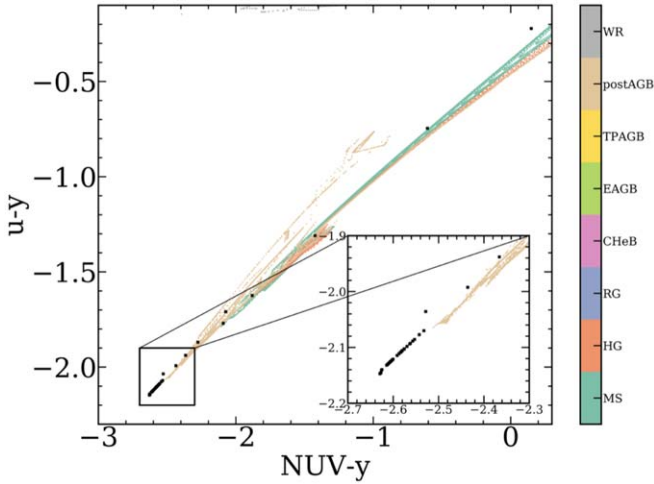

Figure 5. The (NUV − y, u − y) color–color diagram for accreting WD binaries (black squares). In the plot, other dots indicate the isochrones with different ages same as Figure 3. The inset panel shows the data in the black box of the main panel. Different colors in the plot indicate the types of stars. Here we do not show all types of stars in order to clearly show the region with accreting WD binaries.

errors of these colors are smaller than 0.1 dex, we can find that accreting WD binaries with NUV − y ∼ −2.5 and u − y ∼ −2.1 are distinguishable from stars with other types from this plot. The accreting WDs in these binaries have effective temperatures $\log(T_{\rm eff}/{\rm K}) > 5.0$ and $\log(g\,{\rm cm}^{-1}\,{\rm s}^2) > 5.0$. Their WD masses range from $0.60\,M_\odot$ to $1.377\,M_\odot$. The accretion rates of these accreting WDs are close to the accretion rate in the stable burning regime and smaller than $10^{-5}\,M_\odot\,{\rm yr}^{-1}$.

But for other accreting WDs, we cannot distinguish with this color–color diagram. In Figure 6, we show the (NUV − r, u − g), (NUV − i, u − g), (NUV − z, u − g) and (NUV − y, u − g) color–color diagrams for accreting WD binaries. We can find that some accreting WD binaries with colors ∼ −0.5−0 can be distinguished from other stars. These accreting WDs are RAWDs. They have effective temperatures around 10^4 K and accretion rates of 10^{-5}–$10^{-4}\,M_\odot\,{\rm yr}^{-1}$.

4. Discussion

4.1. Accreting WDs in Old Stellar Populations

In Figure 7, we show the (NUV − i, u − g) color–color diagram for accreting WDs in a simple stellar population with an age around $\log_{10}(t/{\rm yr}) = 10$–10.1 Given the old age of this population, only these post-AGB stars have colors close to the accreting WD binaries. From this plot, we can find that most accreting WDs may be easy to be found in this simple stellar population, in particular these accreting WDs with NUV − i ranging from −1.0 to −1.5 (see Figure 6). These results indicate that globular clusters may be a good place to search for accreting WD binaries.

4.2. Impact of Interstellar Medium

In our work, we do not consider the impact of interstellar medium on the spectra of the accreting WDs. Given the high temperatures of accreting WDs, their emission should be capable of ionizing the interstellar medium, producing some emission lines, such as He II λ4686, [O III] λ5007, and [O I] λ6300 (Rappaport et al. 1994). This may also produce a
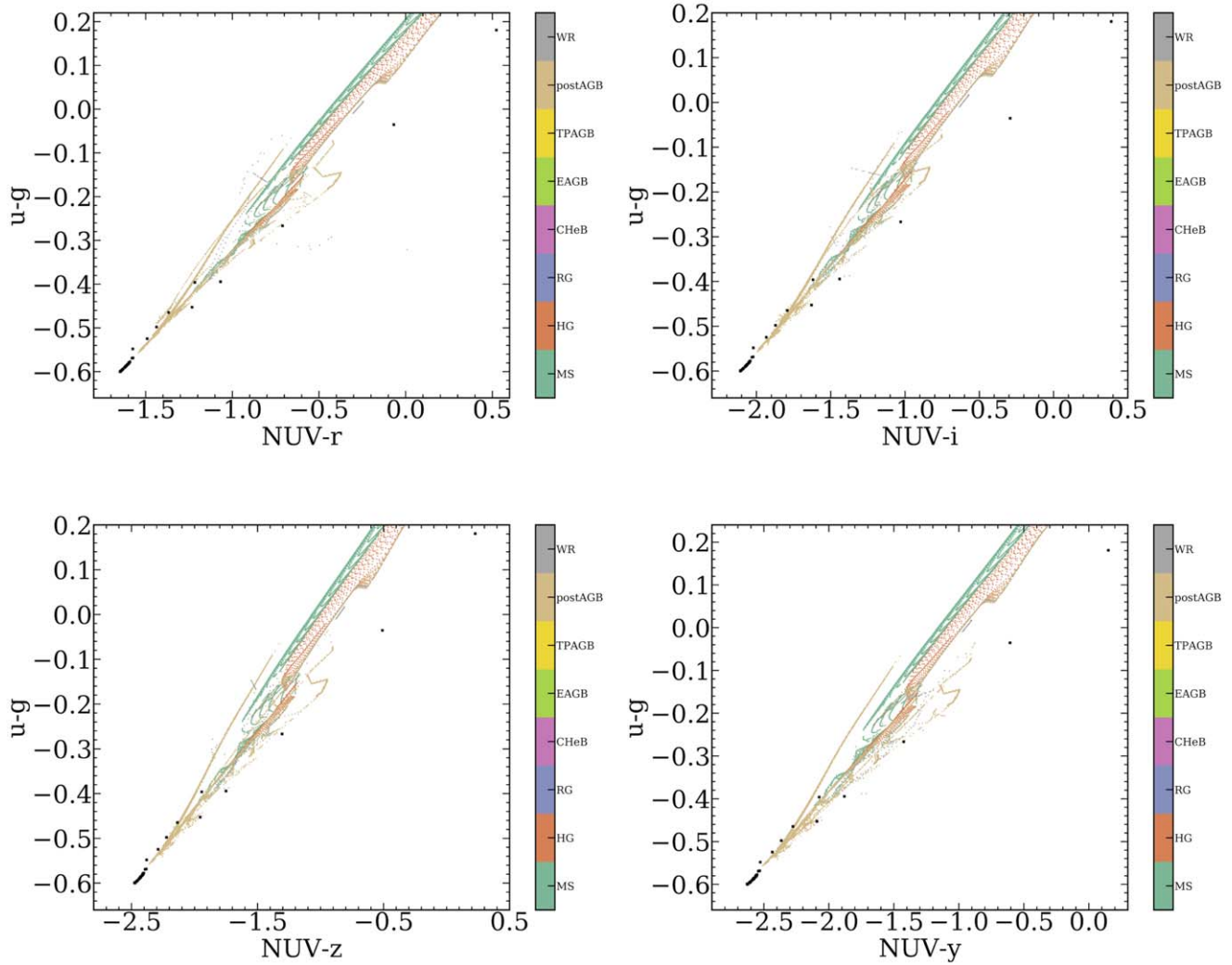
Figure 6. The $(NUV - r, u - g)$, $(NUV - i, u - g)$, $(NUV - z, u - g)$, $(NUV - y, u - g)$ color–color diagrams for accreting WD binaries. The meaning of symbols and colors are the same as Figure 3.
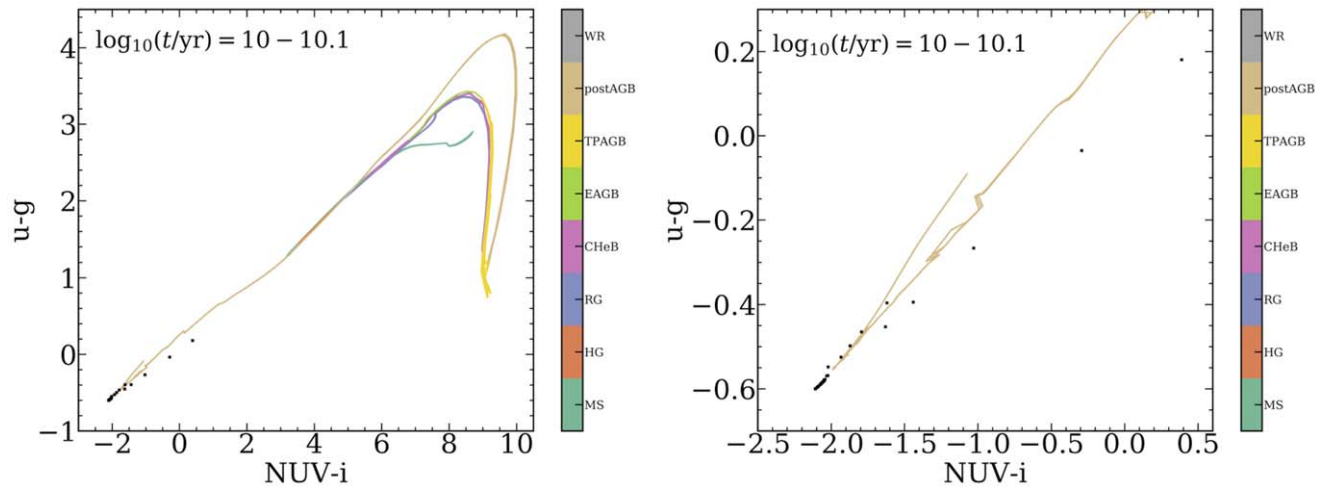

Figure 7. The left panel is the $(NUV - i, u - g)$ color–color diagram for accreting WD binaries (black dots) in a simple stellar population with an age around $\log_{10}(t/yr) = 10\text{-}10.1$. The right panel shows the zooming plot of the down-left corner of the left panel. In these two panels, the colorful dots represent the isochrones with ages from $\log_{10}(t/yr) = 10\text{-}10.1$. Different colors indicate different types of stars.

nebulae around the accreting WD, similar to CAL 83 (Remillard et al. 1995). But Woods & Gilfanov (2016) found that whether an accreting WD has a nebular around it will depend on the density of interstellar medium. If the density of interstellar medium is too low, there will be no nebular around the accreting WD. Moreover, they demonstrated that most supersoft X-ray sources are in low density media. Therefore, we would expect that the interstellar medium might have little impact on our results.

5. Conclusions

In this paper, we have investigated the possibility of searching for accreting WD binaries with the CSST. We have presented their properties, such as $\log g$, $\log T_{\rm eff}$ and $\log L$. In addition, we also present their location on different color–color diagrams. We find that the properties of accreting WD binaries are very different from isolated WDs. We can distinguish these accreting WD binaries with very high or low effective temperatures from stars of other types with $(\mathrm{NUV} - y, \ u - y)$, $(\mathrm{NUV} - r, \ u - g)$, $(\mathrm{NUV} - i, \ u - g)$, $(\mathrm{NUV} - z, \ u - g)$ and $(\mathrm{NUV} - y, \ u - g)$ color–color diagrams. Therefore, we would expect that some accreting WDs can be found by the CSST.

Acknowledgments

References

Amaro-Seoane, P., Audley, H., Babak, S., et al. 2017, arXiv:1702.00786
Cao, Y., Gong, Y., Meng, X.-M., et al. 2018, MNRAS, 480, 2178
Cassisi, S., Iben, I., Jr., & Tornambe, A. 1998, ApJ, 496, 376
Chen, H.-L., Woods, T. E., Yungelson, L. R., et al. 2019a, MNRAS, 490, 1678
Chen, H.-L., Woods, T. E., Yungelson, L. R., Gilfanov, M., & Han, Z. 2014, MNRAS, 445, 1912
Chen, H.-L., Woods, T. E., Yungelson, L. R., Gilfanov, M., & Han, Z. 2015, MNRAS, 453, 3024
Chen, Y., Girardi, L., Fu, X., et al. 2019b, A&A, 632, A105
Choi, J., Dotter, A., Conroy, C., et al. 2016, ApJ, 823, 102
Dotter, A. 2016, ApJS, 222, 8
Gong, Y., Liu, X., Cao, Y., et al. 2019, ApJ, 883, 203
Hachisu, I., & Kato, M. 2003, ApJ, 598, 527
Hachisu, I., Kato, M., & Nomoto, K. 1996, ApJL, 470, L97
Hachisu, I., Kato, M., & Nomoto, K. 1999, ApJ, 522, 487
Han, Z., Podsiadlowski, P., & Eggleton, P. P. 1995, MNRAS, 272, 800
Han, Z., Podsiadlowski, P., Maxted, P. F. L., Marsh, T. R., & Ivanova, N. 2002, MNRAS, 336, 449
Han, Z.-W., Ge, H.-W., Chen, X.-F., & Chen, H.-L. 2020, RAA, 20, 161
Hurley, J. R., Pols, O. R., & Tout, C. A. 2000, MNRAS, 315, 543
Hurley, J. R., Tout, C. A., & Pols, O. R. 2002, MNRAS, 329, 897
Iben, I. J., & Tutukov, A. V. 1986, ApJ, 311, 753
Iben, I., Jr., & Tutukov, A. V. 1984, ApJS, 54, 335
Kahabka, P., & van den Heuvel, E. P. J. 2006, Compact Stellar X-ray Sources, Vol. 39 (Cambridge: Cambridge Univ. Press), 461
Kato, M., & Hachisu, I. 1994, ApJ, 437, 802
Kippenhahn, R., Weigert, A., & Weiss, A. 2012, Stellar Structure and Evolution (Berlin: Springer)
Lepo, K., & van Kerkwijk, M. 2013, ApJ, 771, 13
Li, Z., Chen, X., Chen, H.-L., & Han, Z. 2019, ApJ, 871, 148
Lipunov, V. M., & Postnov, K. A. 1988, Ap&SS, 145, 1
Liu, W.-M., Jiang, L., & Chen, W.-C. 2021, ApJ, 910, 22
Nelemans, G., Yungelson, L. R., & Portegies Zwart, S. F. 2004, MNRAS, 349, 181
Paczynski, B., & Zytkow, A. N. 1978, ApJ, 222, 604
Podsiadlowski, P., Han, Z., & Rappaport, S. 2003, MNRAS, 340, 1214
Postnov, K. A., & Yungelson, L. R. 2014, LRR, 17, 3
Rappaport, S., Chiang, E., Kallman, T., & Malina, R. 1994, ApJ, 431, 237
Rauch, T. 2011, arXiv:1108.6168
Rauch, T., Demleitner, M., Hoyer, D., & Werner, K. 2018, MNRAS, 475, 3896
Rauch, T., Orio, M., Gonzales-Riestra, R., et al. 2010, ApJ, 717, 363
Remillard, R. A., Rappaport, S., & Macri, L. M. 1995, ApJ, 439, 646
Sion, E. M., Acierno, M. J., & Tomczyk, S. 1979, ApJ, 230, 832
Steiner, J. E., & Diaz, M. P. 1998, PASP, 110, 276
Taam, R. E., & van den Heuvel, E. P. J. 1986, ApJ, 305, 235
Tauris, T. M., Sanyal, D., Yoon, S.-C., & Langer, N. 2013, A&A, 558, A39
Tutukov, A. V., & Yungelson, L. R. 1994, MNRAS, 268, 871
van den Heuvel, E. P. J., Bhattacharya, D., Nomoto, K., & Rappaport, S. A. 1992, A&A, 262, 97
Wang, B., & Han, Z. 2012, NewAR, 56, 122
Warner, B. 2003, Cataclysmic Variable Stars (Cambridge: Cambridge Univ. Press)
Wolf, W. M., Bildsten, L., Brooks, J., & Paxton, B. 2013, ApJ, 777, 136
Woods, T. E., & Gilfanov, M. 2016, MNRAS, 455, 1770
Zhan, H. 2011, SSPMA, 41, 1441